Journal of Materials Science: Materials in Electronics (2020) 31:16759–16768
https://doi.org/10.1007/s10854-020-04231-8

Efficiency enhancement in dye-sensitized solar cells through the decoration of electro-spun TiO_2 nanofibers with Ag nanoparticles

Atiye Moradi[1] · Masoud Abrari[2] · Morteza Ahmadi[2]

Received: 31 May 2020 / Accepted: 11 August 2020 / Published online: 19 August 2020

Abstract
Dye-sensitized solar cells (DSSCs) are low cost and eco-friendly photovoltaic devices which require new ideas for further development. In this paper, we use electro-spun TiO_2 nanofibers to prepare the DSSCs photoanode. In order to isolate the FTO and electrolyte species, we deposit a spin-coated TiO_2 blocking layer at their interface. The performance of this cell is further improved by introducing surface plasmon resonances (SPRs) at the surface of the nanofibers. It is shown that SPRs increase the generated current in the cells by providing a higher light absorption and lower recombination. Our best cell showed an efficiency of 6.19%, which is a 28% improvement in comparison to the bare DSSC with 4.84% efficiency. The results of this paper are acquired and confirmed by XRD, FESEM, TEM, EDS, dye-loading, IPCE, *J*–*V*, and EIS measurements.

1 Introduction

Solar energy is, without any doubt, a clean and sustainable source of energy that provides mankind with a high amount of light and heat every day. Photovoltaic devices or solar cells that directly convert the incoming light into electricity are considered as an excellent method for utilization of solar energy [1, 2]. Among these devices, dye-sensitized solar cells (DSSCs) show a promising horizon due to their eco-friendliness, low cost, and high efficiency [3, 4].

In recent years, many studies have been conducted on DSSCs, and efficiencies of up to ~ 13% have been attained [4, 5]. Yet, this amount can be further improved by employing new ideas which mostly focus on replacing or modification of common DSSCs' components such as using organic counter electrodes [6] or dyes [7], changing the redox mediator [8] or modification of TiO_2 with various semiconductors, metals, non-metals, hybridization with graphene or carbon nanotubes, and plasmonic nanoparticles [9–12].

An excellent method for improving the performance of DSSCs is to introduce surface plasmon resonances (SPRs) to their surface [13]. SPRs are formed at the interface between a metal and a medium with negative and positive dielectric constants, respectively [14]. By this means, the shortfalls of the TiO_2 layers that are poor charge transport and high electron recombination can be addressed due to the suitable transport pathway provided by the SPRs and the recombination at TiO_2/dye and dye/electrolyte interface can be minimized [15, 16]. Furthermore, the properties of the TiO_2 photoanode can also be enhanced through composition with nanostructures such as nanorods, nanofibers, nanotubes, and nanowires, which possess large surface areas and unidirectional electron allocation also increase charge transport pathways [9, 17, 18].

In this paper, to achieve a higher performance DSSC, we first prepare blocking layer/nanofiber composite photoanodes through the electrospinning and spin coating methods and then decorate them with different ratios of silver (Ag) nanoparticles to create SPRs. We believe that by employing the block layer/nanofiber structure at the same time with surface plasmon resonances, more suitable electron pathways are created, which minimizes the recombination and improves the overall DSSC performance.

✉ Morteza Ahmadi
seyedmortezaahmadi@gmail.com

Atiye Moradi
atiemoradi@gmail.com

Masoud Abrari
masoud.abrari@gmail.com

[1] Department of Chemistry, Faculty of Physics & Chemistry, Alzahra University, Vanak, P.O. Box 1993891176, Tehran, Iran

[2] Laser and Plasma Research Institute, Shahid Beheshti University, G.C., Evin, 1983969411, Tehran, Iran

2 Experiment

In this study, all the chemical materials are purchased from Merck Co. with analytical grade unless mentioned otherwise. In order to prepare TiO_2 nanofibers, we employed the electrospinning technique. For this purpose, 10 g of titanium (IV) isopropoxide (TTIP) was dispersed in 70 mL of analytical grade ethanol (Amertat Shimi Co.) on a magnetic stirrer with 70 °C temperature. 4 g of polyvinylpyrrolidone with 1,300,000 molar weight (PVP1300000) along with 20 mL acetic acid was added to the solution and stirred for 4 h so that a homogenous sol is acquired. The resulting sol was transferred into a syringe with a 22-gauge needle and placed in an electrospinning system with 10 kV voltage and at a distance from the collector of 10 cm. The process was conducted on an aluminum foil substrate for 30 min, and the deposited film was calcined at 500 °C for 1 h to remove the organics and for crystallization.

Since the nanofibers have a porous structure, they cannot provide suitable isolation between the electrolyte and FTO interface, and thus, a blocking layer is necessary. To prepare the TiO_2 blocking layer, 730 µL of titanium (diisopropanol)bis(2,4-pentanedione) was dissolved in 10 mL of ethanol on a magnetic stirrer and then spin-coated on FTO for 3 rounds of 3000 rpm. The prepared film was also annealed at 500 °C for 1 h. In order to prepare a paste from the nanofibers, they were dispersed in ethanol and stirred for 30 min. Ethylene glycol and Terpineol were added to the solution and stirred for another 1 h. Three drops of Triton X-100 were also poured into the mixture and heated at 80 °C for 2 h until a composite with high viscosity was acquired. The paste was doctor-bladed on the blocking layers and calcined for 30 min at 500 °C. For decoration of the nanofibers with Ag nanoparticles, the prepared layers were soaked in $AgNO_3$ solutions with 0, 50, 100, and 150 mM concentrations and UV-treated to form Ag-decorated TiO_2 nanofiber photoanodes. These photoanodes were dyed in N719 dye and ethanol solution for 24 h and were subsequently washed with ethanol to remove the extra dye. The DSSCs' structure was completed by Pt-coated FTO counter electrodes and iodide–3 iodide electrolyte. In order to confirm the repeatability of the samples and to conduct statistical analysis, we fabricated up to 20 of each DSSC and provided their average results.

In order to analyze the crystallographic properties of the samples, we used an STOE STADI-P X-ray diffractometer (XRD). The morphological analysis of the samples was carried out by a Mira III, TeScan field emission electron microscope (FESEM) along with a Zeiss-EM10C-100 kV transmission electron microscope (TEM). We employed an Oxford Xmax-80 energy dispersive spectrometer (EDS) to gain information of the elemental distribution. The photovoltaic characteristics of the DSSCs were analyzed by the Sharif Solar sun simulator with its IV tracer. In order to further investigate the photovoltaic properties, we used a Sharif Solar IPCE-018 incident photon to current efficiency (IPCE) measurement system. The electrochemical impedance spectroscopy (EIS) was performed with a Sharif Solar PGE-18 instrument.

3 Results and discussion

Figure 1 illustrates the XRD spectra of the photoanodes dipped in different concentrations of the $AgNO_3$ solution. The peaks at $2\theta = 25.36°$, 37.97°, 48.06°, 54.13°, 55.12°, 62.90°, and 75.24° witnessed in all the samples show perfect correspondence with the JCPDS 01-073-1764 reference card which demonstrates TiO_2 anatase phase. These angles are equivalent to 101°, 004°°, 200°, 105°, 211°, 204°, and 215° crystallographic planes of TiO_2 [19]. We clearly see in these spectra that Ag treatment has not caused any significant alteration on the crystallinity of the TiO_2 nanofibers. In the first place, this shows that Ag treatment does not affect the nanofibers crystallinity and also indicates the low crystallographic properties of Ag nanoparticles. By calculating the crystallite size of the nanofibers through the Debye–Scherrer formula [20], we estimate a crystallite size of around 40 nm for the electro-spun TiO_2 nanofiber, which is a suitable amount in cases of electrical and optical properties [21].

In order to investigate the morphology of the prepared samples, we employed FESEM analysis. Figure 2 shows the FESEM images of the TiO_2 nanofiber photoanodes treated with the $AgNO_3$ solution with 0- and 100-mM concentrations. It is evident in the figure that the nanofibers are appropriately formed in the 0 mM photoanode (Fig. 2a), and their diameter can be assessed to be in the range of 60 to 100 nm. After the treatment with 100 mM concentration $AgNO_3$ solution (Fig. 2b), we observe that Ag nanoparticles are randomly located on the nanofibers' surface. Furthermore, it is seen in the figure that there are aggregations of Ag nanoparticles at some places, but the overall Ag nanoparticle distribution can be considered uniform. To confirm the elemental composition of the samples, we studied them with EDS, which its results for 0, 50, 100, and 150 mM samples are illustrated in Fig. 3. It is evident from EDS analysis that the photoanodes are made from pure Ti and O elements with low amounts of Ag, which signifies the purity of the prepared materials. It is also seen that the Ag content increases in the samples dipped in higher concentrations of the $AgNO_3$ solution. This shows that the concentration has a direct relation with Ag nanoparticle decoration on the surface of the nanofibers. In order to acquire the elemental distribution of the Ag nanoparticles on the prepared nanofibers, we used

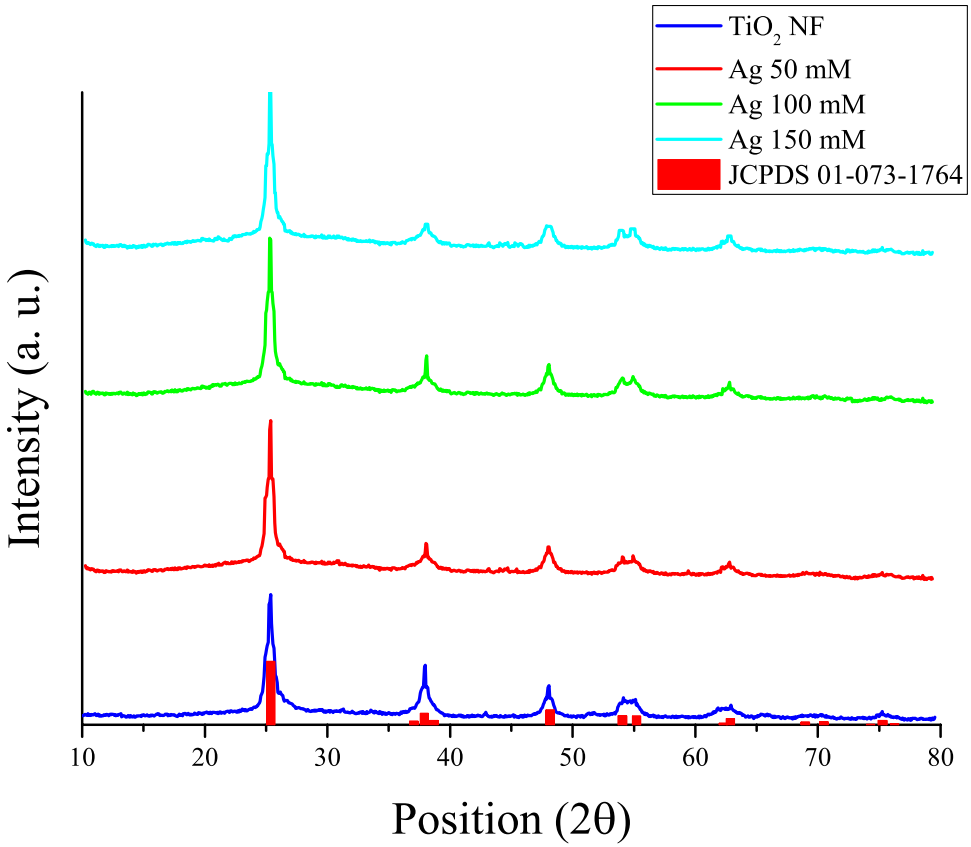

Fig. 1 The XRD spectra of the prepared TiO_2 nanofiber-based photoanodes dipped in different concentrations of $AgNO_3$ solution

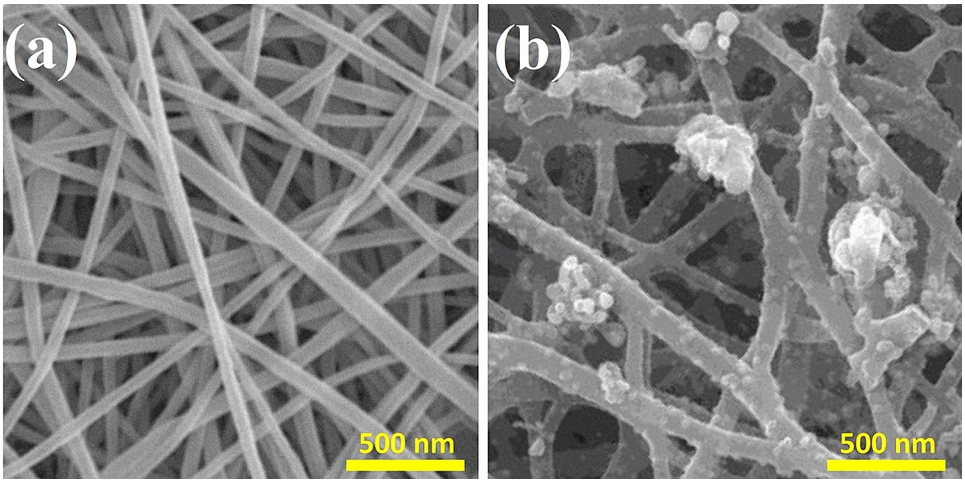

Fig. 2 FESEM images of TiO_2 nanofibers **a** without Ag treatment and **b** with Ag treatment in 100 mM solution

EDS mapping analysis that its results are illustrated in Fig. 4. The homogenous distribution of materials is quite evident in the figures. Figure 4a, which illustrates the mapping results of prepared nanofibers without Ag decoration, shows a uniform distribution for titanium and oxygen elements. In Fig. 4b, we witness that by soaking the prepared nanofibers in $AgNO_3$ solution, Ag nanoparticles are decorated on their outer surface. This clearly illustrate the success in the intended process.

For a more in-depth morphological analysis of the samples, we acquired TEM images from the specimens, which its results for the samples with 0- and 100-mM Ag concentrations are, respectively, shown in Fig. 5a and b. The formation of TiO_2 nanofibers is visible in Fig. 5a, and we observe that Ag nanoparticle colonies are decorated on these nanofibers in Fig. 5b. From this figure, we can also deduce that the Ag-treated nanofibers' outer surface has a higher roughness in comparison with the untreated samples. This

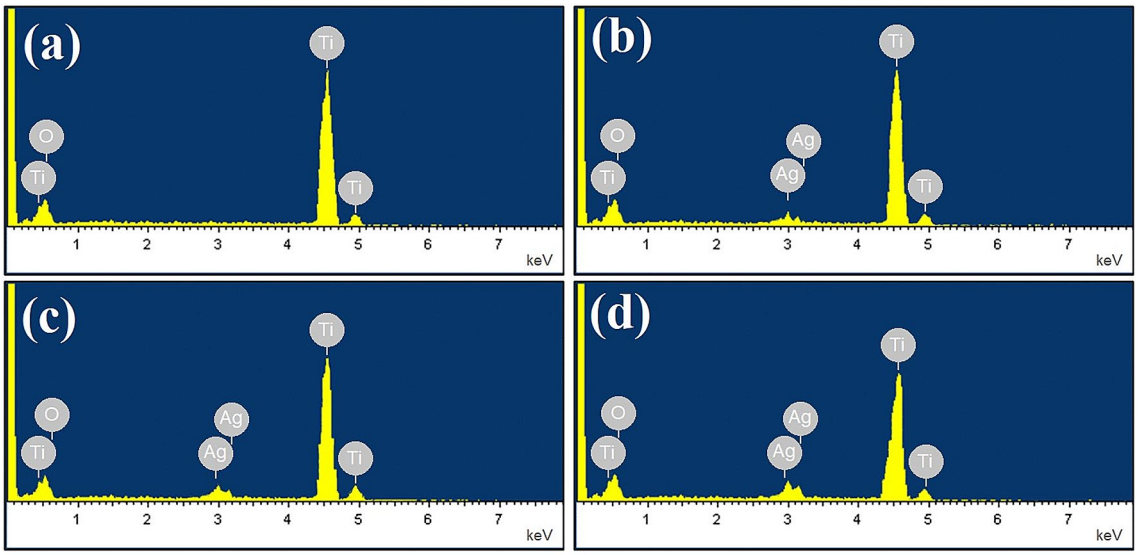

Fig. 3 EDS analysis of the prepared samples dipped in $AgNO_3$ solution with **a** 0, **b** 50, **c** 100, and **d** 150 mM concentrations

higher roughness produces a higher active surface area, which is suitable for DSSC's photoanodes [22].

The electrical and photovoltaic performance of the fabricated DSSCs was investigated by *J*–*V* measurement, which their results are shown in Fig. 6 and Table 1. We see in these results that at first, by increasing the concentration of the $AgNO_3$ solution, the short circuit current density (J_{SC}) increases to 11.24 mA/cm^2 for the cell prepared with 100 mM solution and then drops to 10.61 mA/cm^2 for 150 mM solution. Thus, the DSSC made from an $AgNO_3$ solution with 100 mM concentration demonstrates the highest photovoltaic performance by having a J_{SC} of 11.24 mA/cm^2, an open-circuit voltage (V_{OC}) of 798 mV, and a fill factor (FF) of 69%, which gives an efficiency of 6.19% that is the best amount among the fabricated DSSCs. This high efficiency can be attributed to the increased current density since the V_{OC} of DSSCs doesn't show a substantial change and is in the range of 792 to 798 mV for all the cells. On the other hand, the FF of the cells also is not significantly altered by the Ag treatment and stands between 66 and 69% for all the samples and is not determinantal in the overall efficiency. Therefore, the increase in efficiency is totally due to the increased $J_{SC,}$ which itself may have two reasons: (1) The suitable amount of Ag nanoparticles decorated on TiO_2 nanofibers surface creates plasmonic resonances which integrate the electrical field in the vicinity of the Dye molecules and increases both the dye adsorption and electron–hole generation which improves the current produced by the DSSC [23]. (2) The increased active surface area due to the Ag nanoparticles also improves the dye adsorption, which is also helpful in the improvement of current [24]. As we can see from Fig. 6 and Table 1, after increasing the Ag concentration from 100 to 150 mM, the DSSC's current density and, subsequently, its efficiency witnesses a sharp decrease to 10.61 mA/cm^2 and 5.82%, respectively. This is probably due to the charge trapping effect of the Ag aggregations on the surface of TiO_2 nanofiber, which creates recombination centers and causes a drop in current density.

To confirm the effect of Ag treatment on the dye adsorption of the photoanodes, we employed the dye-loading analysis. For this purpose, a 0.1 M NaOH solution was prepared, and the photoanodes were dipped inside them so that they desorb the loaded dye. Using a UV–Vis spectrometer, we detected the optical transmission of the desorbed dye from the samples, and the results are shown in Fig. 7. In this analysis, the peak located at the wavelength of around 510 nm is attributed to the N719 dye and demonstrates a quantitative measure for the dye adsorption [25]. As we can see from the figure, the dye-loading of the cell dipped in 150 mM $AgNO_3$ solution has the highest, and the cell with no Ag treatment has the lowest amount. To provide a better quantitative result of the dye adsorption, we employed a calibrated curve using a known concentration of N719 dye, in which the results are summarized in Table 1. As we see in the table, by increasing the concentration of $AgNO_3$ solution and the growth of Ag nanoparticles on the surface of TiO_2 nanofibers, the loaded dye increases from 0.82×10^{-7} to 1.52×10^{-7} mol/cm^2. Although the higher amount of dye adsorption is often favorable and useful in the increase of current density, too much dye adsorption creates recombination centers and reduces the produced current. Therefore, the dye adsorption and SPRs at the Ag nanoparticles sites create a trade-off that determines the photovoltaic properties, and thus, the Ag concentration requires an optimization.

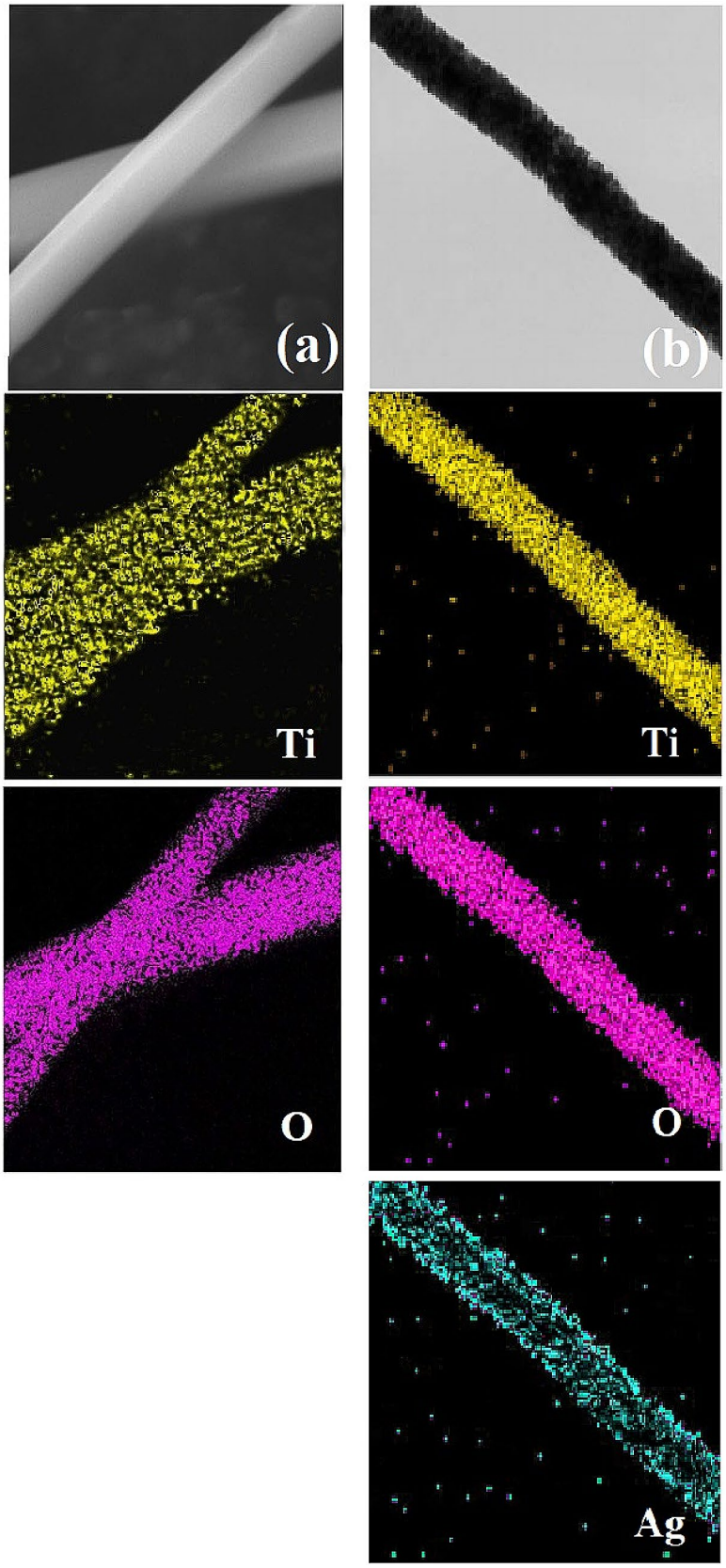

Fig. 4 EDS elemental mapping results of the samples **a** without Ag decoration and **b** decorated with an Ag solution of 100 mM solution

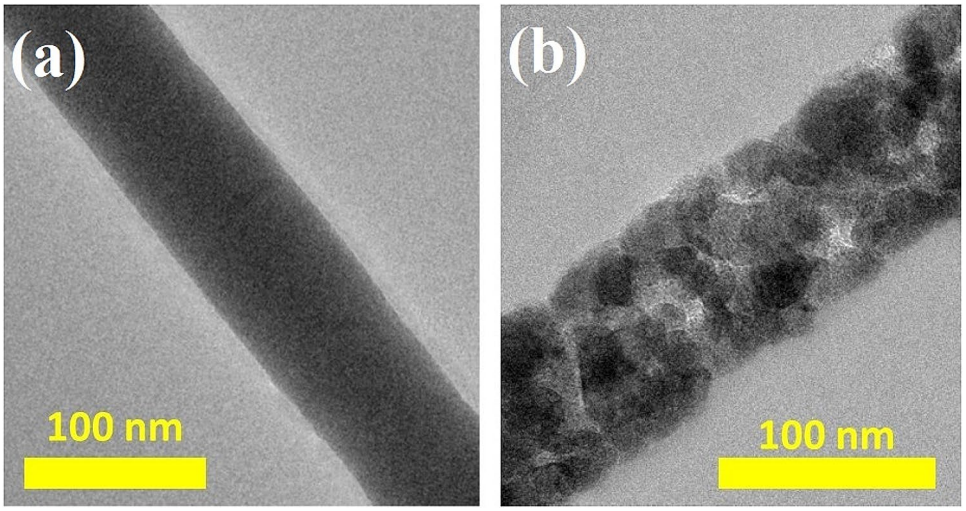

Fig. 5 TEM images of TiO_2 nanofibers **a** without Ag treatment and **b** with Ag treatment in 100 mM solution

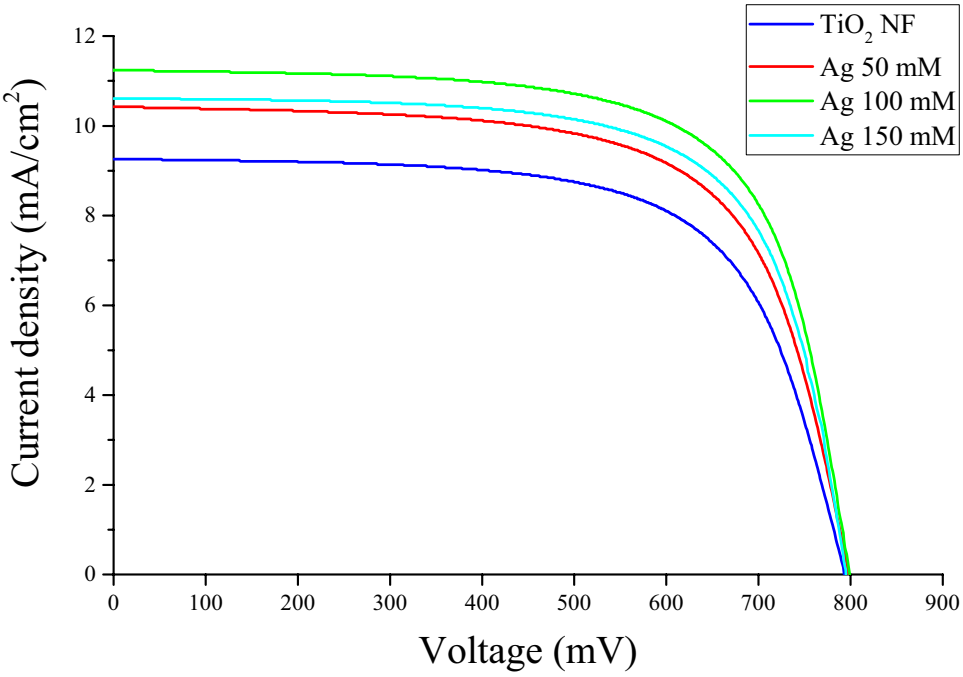

Fig. 6 *J–V* characteristic curves of the fabricated DSSCs dipped in different ratios of $AgNO_3$ solution

Table 1 photovoltaic parameters of the cells assembled with different $AgNO_3$ treatment

Cell	V_{OC} (mV)	Standard deviation (mV)	J_{SC} (mA/cm^2)	Standard deviation (mA/cm^2)	FF	Standard deviation	PCE (%)	Standard deviation (%)	Dye-loading ($\times 10^{-7}$ mol/cm^2)
TiO_2 NF	792	6.3	9.26	0.05	0.66	0.010	4.84	0.14	0.82
Ag 50 mM	797	3.5	10.42	0.05	0.67	0.007	5.56	0.09	1.28
Ag 100 mM	798	5.8	11.24	0.06	0.69	0.008	6.19	0.13	1.40
Ag 150 mM	795	4.0	10.61	0.05	0.69	0.009	5.82	0.12	1.52

Figure 8 displays the IPCE diagrams of DSSCs fabricated from TiO_2 nanofibers and sensitized by N719 dye with different concentrations of Ag treatment. In these spectra, the ratios of incident light converted to electrons at each wavelength are clear. As we can see in the figure, in all the samples, there is a peak in the wavelength range of 500 to

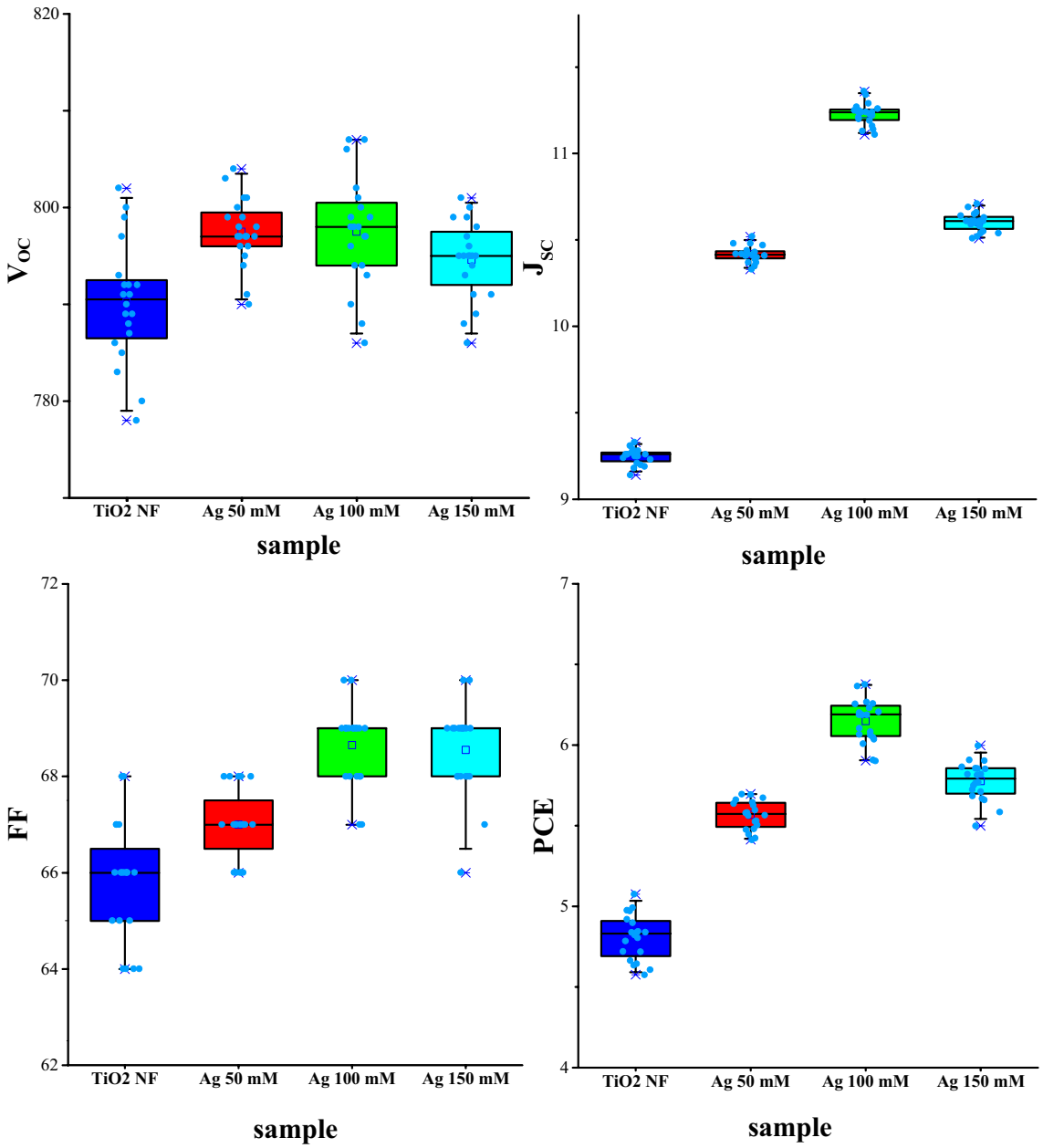

Fig. 7 Box and Whisker diagrams of the fabricated DSSCs

600 nm, which is due to the N719 dye adsorption. The height of this peak has the highest value for the cell treated with 100 mM $AgNO_3$ solution, and we see a 32% increase in comparison with the untreated cell. This means that a higher current is generated in this cell, and the higher efficiency of this DSSC is justifiable.

For a more comprehensive analysis of the charge transport properties in fabricated DSSCs, we performed EIS measurement on them. In this analysis, the DSSCs are placed in the dark situation and were swept by a perturbing signal of 10 mV in the 0.1 to 1 MHz frequency range while recording their impedance behavior. The results of this analysis are illustrated in the Nyquist diagrams of Fig. 8 for the DSSCs treated by $AgNO_3$ solution with 0, 50, 100, and 150 mM concentrations. In all of these diagrams, we observe 2 semicircles located at different frequency ranges. The right semicircle at mid-range frequency attributes to the electron transfer between TiO_2 nanofibers, electrolyte species, and dye molecules. The smaller semicircle at higher frequencies is due to the combined share of electron transport between the counter electrode and electrolyte and also between FTO and TiO_2

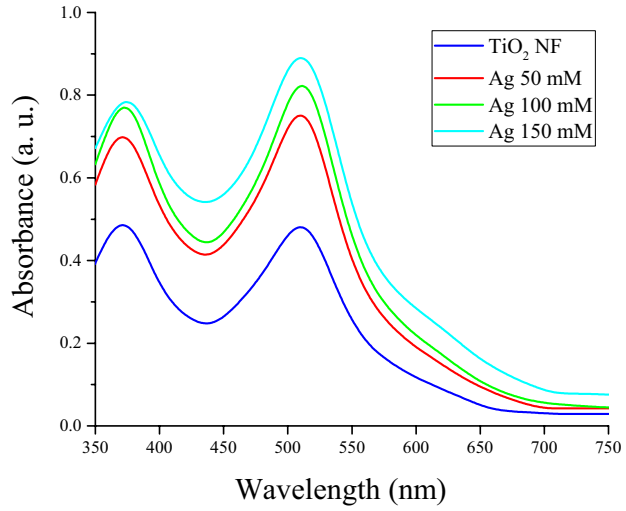

Fig. 8 Absorbance spectra of the prepared samples in dye-loading analysis

[20]. We may also witness the third semicircle at very low frequencies, which is caused by electron transfer by the electrolyte species, but this can be neglected through appropriate electrolyte concentration. In other words, this value, which is called Warburg impedance, has a low importance in DSSCs and can be addressed by the electrolyte concentration. The extracted values from the Nyquist diagram, which are acquired by the Zview software and the fitted equivalent circuit, are shown in Fig. 9 and Table 2. As we can see, the series resistance (R_S) in all the cells is between 8 to 11 Ω which doesn't reflect a meaningful difference and thus shows that all the DSSCs are fabricated with the same parameters in this regard. Furthermore, the

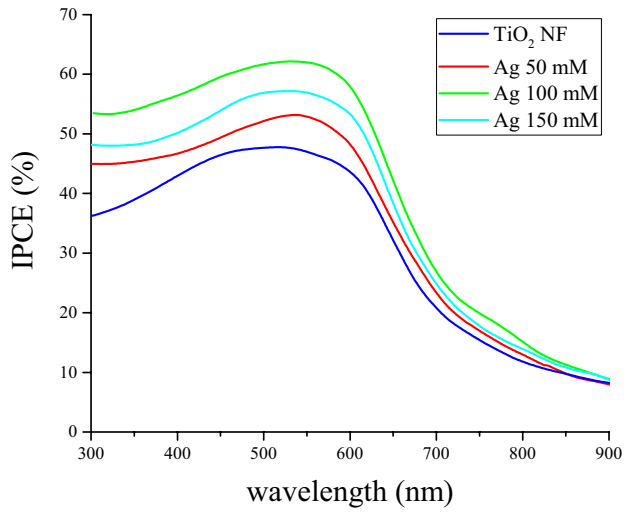

Fig. 9 IPCE diagrams of the fabricated DSSCs with different Ag nanoparticle concentrations

Table 2 Extracted parameters from Nyquist diagrams of the cells fabricated with different $AgNO_3$ treatment

Cell	R_s (Ω)	R_{ct1} (Ω)	R_{ct2} (Ω)
TiO_2 NF	11.0	8.7	115
Ag 50 mM	10.1	8.1	130
Ag 100 mM	10.0	6.2	145
Ag 150 mM	8.8	9.4	135

amount of R_{ct1} which shows the charge transfer resistance between the counter electrode and electrolyte and also between FTO and TiO_2 nanofibers is also the same and between 8 to 10 Ω for all the DSSCs which is due to the TiO_2 blocking layer and the same counter electrode for all the cells. The R_{ct2} value, which in dark situation is directly related to the recombination [26], is 115, 130, 145, and 135 Ω for the DSSCs treated with $AgNO_3$ solution with concentrations of 0, 50, 100, and 150 mM, respectively. In this situation, electrons are transported from FTO to TiO_2 and are recombined with the electrolyte species near the interface. Thus, the charge transfer resistance (R_{ct2}) is mostly composed of $R_{recombination}$. As we can see from the EIS results in Table 2, the cell dipped in the Ag concentration of 100 mM has the highest charge transfer resistance, which is equivalent to the lowest recombination between electrons and the electrolyte species which result in the higher current. Therefore, the EIS analysis confirms the previous J-V and IPCE analyses, and a concentration of 100 mM of $AgNO_3$ solution is the optimized value for fabricating Ag nanoparticle-enhanced SPR DSSCs based on TiO_2 nanofibers (Fig. 10).

4 Conclusion

In summary, we prepared TiO_2 nanofibers using the electrospinning method and fabricated DSSCs from them. In order to isolate the FTO from the electrolyte, we deposited a TiO_2 blocking layer on FTO. To further enhance the photovoltaic properties, we employed SPR phenomena into DSSC using Ag nanoparticles. Different concentrations of the $AgNO_3$ solution were investigated so that the number of nanoparticles decorated on TiO_2 nanofibers is optimized. Our best DSSC, which was dipped in 100 mM $AgNO_3$ solution, demonstrated a dramatic efficiency increase of 28% in comparison with the bare cell. This efficiency enhancement is attributed to the increased current in the cell, which is the result of improved dye adsorption and lower recombination caused by the SPRs at the Ag/nanofibers interface. The method used in this study shows promising results for further enhancing the DSSC's performance in the future.

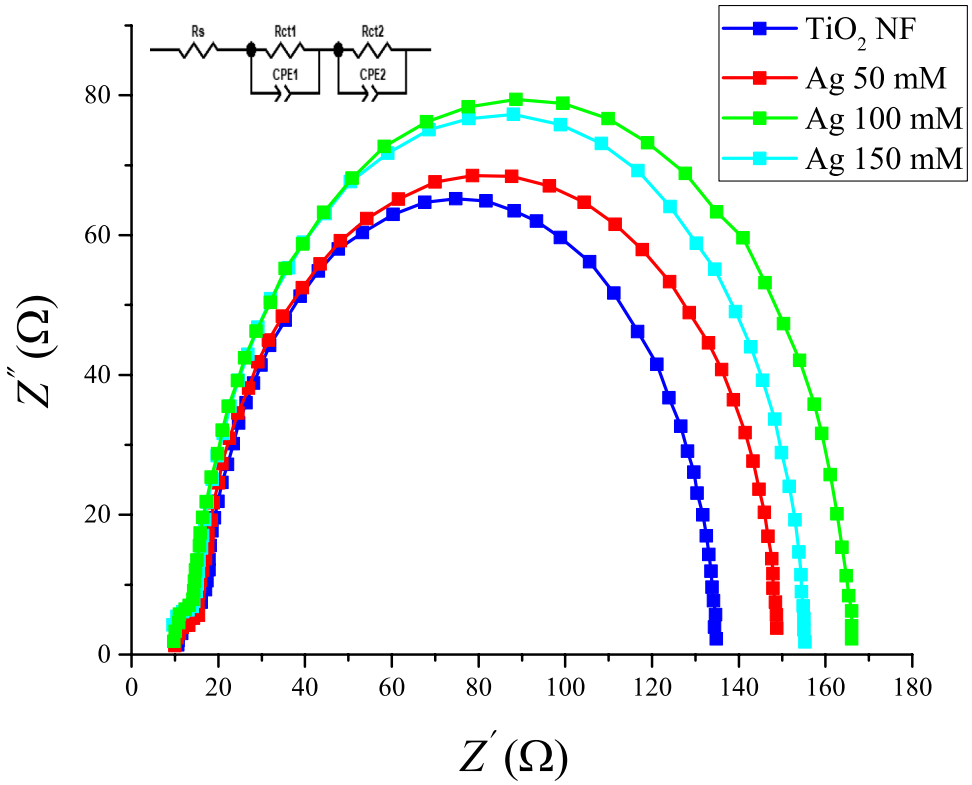

Fig. 10 EIS measurement of the prepared photoanodes with different Ag concentrations and (inset) the equivalent circuit

References

1. J. Day, S. Senthilarasu, T.K. Mallick, Improving spectral modification for applications in solar cells: a review. Renew. Energy **132**, 186–205 (2019)
2. S. Mohammadnejad, A. Khalafi, S.M. Ahmadi, Mathematical analysis of total-cross-tied photovoltaic array under partial shading condition and its comparison with other configurations. Sol. Energy **133**, 501–511 (2016)
3. D.K. Kumar et al., Functionalized metal oxide nanoparticles for efficient dye-sensitized solar cells (DSSCs): a review. Mater. Sci. Energy Technol. **3**, 472–481 (2020)
4. P. Semalti, S.N. Sharma, Dye sensitized solar cells (DSSCs) electrolytes and natural photo-sensitizers: a review. J. Nanosci. Nanotechnol. **20**(6), 3647–3658 (2020)
5. S. Zainudin, H. Abdullah, M. Markom, Electrochemical studies of tin oxide based-dye-sensitized solar cells (DSSC): a review. J. Mater. Sci.: Mater. Electron. **30**(6), 5342–5356 (2019)
6. A. Zatirostami, A new electrochemically prepared composite counter electrode for dye-sensitized solar cells. Thin Solid Films (2020). https://doi.org/10.1016/j.tsf.2020.137926
7. S. Shalini et al., Status and outlook of sensitizers/dyes used in dye sensitized solar cells (DSSC): a review. Int. J. Energy Res. **40**(10), 1303–1320 (2016)
8. H. Kusama, Interaction of tris (4-anisyl) amine mediator in dye-sensitized solar cells. J. Photochem. Photobiol. A **387**, 112150 (2020)
9. Y.-H. Nien et al., Investigation of dye-sensitized solar cell with photoanode modified by TiO_2-ZnO nanofibers. IEEE Trans. Semicond. Manuf. **33**(2), 295–301 (2020)
10. Q. Liu, J. Wang, Dye-sensitized solar cells based on surficial TiO_2 modification. Sol. Energy **184**, 454–465 (2019)
11. H.M.A. Javed et al., Investigation on the surface modification of TiO_2 nanohexagon arrays based photoanode with SnO_2 nanoparticles for highly-efficient dye-sensitized solar cells. Mater. Res. Bull. **109**, 21–28 (2019)
12. M.M. Theint et al., Effect of photoanode modification on charge transport, recombination and efficiency of dye sensitized solar cells using synthetic organic dyes. J. Mater. Sci. Eng. A **10**(1–2), 30–36 (2020)
13. Q. Liu et al., Au@ Ag@ Ag_2S heterogeneous plasmonic nanorods for enhanced dye-sensitized solar cell performance. Sol. Energy **185**, 290–297 (2019)
14. J.-Y. Jing et al., Long-range surface plasmon resonance and its sensing applications: a review. Opt. Lasers Eng. **112**, 103–118 (2019)
15. R.J. Beula, D. Suganthi, A. Abiram, TiO_2 photo-electrode with gold capping for improved observation in dye-sensitized solar cell. Appl. Phys. A **126**(3), 1–8 (2020)
16. T. Solaiyammal, P. Murugakoothan, Green synthesis of Au and the impact of Au on the efficiency of TiO_2 based dye sensitized solar cell. Mater. Sci. Energy Technol. **2**(2), 171–180 (2019)
17. S. Vinoth et al., Enhanced ionic conductivity of electrospun nanocomposite (PVDF-HFP+ TiO_2 nanofibers fillers) polymer fibrous membrane electrolyte for DSSC application. Polym. Compos. **40**(4), 1585–1594 (2019)
18. Y. Deng et al., Improved photoelectric performance of DSSCs based on TiO_2 nanorod array/Ni-doped TiO_2 compact layer composites film. J. Solid State Electrochem. **23**(11), 3031–3041 (2019)
19. P. Santos-Aguilar, F.F. Contreras-Torres, X-ray diffraction line profile analysis: a microstructural study in polymorphic TiO_2. Mater. Today: Proc. **13**, 420–427 (2019)
20. M. Saeidi, M. Abrari, M. Ahmadi, Fabrication of dye-sensitized solar cell based on mixed tin and zinc oxide nanoparticles. Appl. Phys. A **125**(6), 409 (2019)
21. S. Umale et al., Improved efficiency of DSSC using combustion synthesized TiO_2. Mater. Res. Bull. **109**, 222–226 (2019)

22. Q. Wali et al., SnO_2–TiO_2 hybrid nanofibers for efficient dye-sensitized solar cells. Sol. Energy **132**, 395–404 (2016)
23. A. Pandikumar et al., Titania@ gold plasmonic nanoarchitectures: an ideal photoanode for dye-sensitized solar cells. Renew. Sustain. Energy Rev. **60**, 408–420 (2016)
24. R. Kumar et al., Zinc oxide nanostructure-based dye-sensitized solar cells. J. Mater. Sci. **52**(9), 4743–4795 (2017)
25. X. Dou et al., Zn-doped SnO_2 nanocrystals as efficient DSSC photoanode material and remarkable photocurrent enhancement by interface modification. J. Electrochem. Soc. **159**(9), H735 (2012)
26. J. Zhao et al., Efficient light-scattering functionalized TiO_2 photoanodes modified with cyanobiphenyl-based benzimidazole for dye-sensitized solar cells with additive-free electrolytes. J. Mater. Chem. **22**(35), 18380–18386 (2012)